Aerosol characterisation at the FEBUKO upwind station Goldlauter (I): Particle mass, main ionic components, OCEC, and mass closure

T. Gnauk[a],[*], E. Brüggemann[a], K. Müller[a], R. Chemnitzer[a], C. Rüd[a],
D. Galgon[a], A. Wiedensohler[a], K. Acker[b], R. Auel[b], W. Wieprecht[b], D. Möller[b],
W. Jaeschke[c], H. Herrmann[a]

[a]*Leibniz-Institut für Troposphärenforschung e.V., Permoserstr. 15, D-04318 Leipzig, Germany*
[b]*Brandenburgisch-Technische Universität, Abt. Luftchemie, Volmerstr. 13, D-12489 Berlin, Germany*
[c]*Zentrum für Umweltforschung der Johann Wolfgang Goethe-Universität, Georg-Voigt-Str. 14, D-60325 Frankfurt, Germany*

Abstract

This contribution presents characterisation efforts of the gas phase and particle phase main components during the FEBUKO orographic cloud passage experiments in autumn 2001 and 2002 in the Thüringer Wald (Germany). Three events out of a total of 14 were chosen as the best events considering all meteorological conditions. Gas phase and size-segregated particle phase data obtained from physical (dry size distribution) and chemical (particle mass, main ions, OCEC, and water-soluble metals) measurements are presented for the upwind site. The total particulate mass concentration (PM_{10}) was found to be between 8 and $17 \, \mu g \, m^{-3}$. Particles with an aerodynamic diameter up to $1.2 \, \mu m$ contribute about 80% of the mass concentration. About 90% of the total ion concentration consists of nitrate, sulphate and ammonium. The OC concentration in all three events amounts to about $1.0 \, \mu g \, m^{-3}$, whereas EC concentrations were between 0.40 and $1.0 \, \mu g \, m^{-3}$. The contribution of OC and EC to stage mass ranged from 5% to 35% and from 2% to 17%, respectively. The water content of particles was estimated to be 16–18%. Physical and chemical mass closure is discussed in detail and the results are in a reasonable agreement. The complex data set obtained for each event can be used in the initialisation of models for the multiphase processes during and after the cloud passage of the characterised air mass.

© 2005 Elsevier Ltd. All rights reserved.

Keywords: Size-segregated particle characterisation; Major ions; OCEC; Physical and chemical mass closure

1. Introduction

The atmospheric aerosol plays an important role in the trace material cycle of the atmosphere and may influence radiation forcing and atmospheric chemistry. Aerosols can also act as condensation nuclei in the cloud formation. Formed clouds continuously process particles and thus modify their chemical composition (Hallberg et al., 1994; Kreidenweis et al., 2003; Hegg et al., 2004). Therefore, it is particularly important to determine the size-segregated physical and chemical properties of the atmospheric aerosol. At present, only a

---

*Corresponding author. Tel.: +49 341 235 2156;
fax: +49 341 235 2325.

E-mail address: gnauk@tropos.de (T. Gnauk).

limited number of studies are available measuring size-segregated particle composition with emphasis on organic species in Europe (e.g. Nunes and Pio, 1993; Mészáros et al., 1997, 1998; Neusüß et al., 2000a, b, 2002; Maenhaut et al., 2002; Pakkanen et al., 2003; Bardouki et al., 2003; Lammel et al., 2003; Plewka et al., 2004).

Size-segregated aerosol sampling and characterisation at the upwind site of the summit (Mount Schmücke) was part of the FEBUKO/MODMEP research projects within the German Atmospheric Research Programme AFO 2000 Programme (www.afo-2000.de). The main goal of the FEBUKO field studies was to put a basis for the further development of tropospheric cloud chemistry models. A complex experimental data set was obtained by two field campaigns in 2001 and 2002. This data set was used as a realistic initialisation dataset for the newly developed applied models (SPACCIM, CAPRAM 3.0). The model calculations are capable of reproducing the flow of the approaching air mass from the upwind site above the summit with its orographic cloud to the downwind site. The air masses of the experimental region were typically from an anthropogenic influenced origin which has been exposed to biogenic emissions on their way from the Rhein-Main area to the Thüringer Wald. For a more detailed description and results of the FEBUKO experiments see Herrmann et al. (2005a), Brüggemann et al. (2005), van Pinxteren et al. (2005), Tilgner et al. (2005b).

2. Experimental set-up

Aerosol sampling was performed at the upwind site in the village of Goldlauter (U site, 605 m asl, 10°45′20″E, 50°38′25″N), Thüringer Wald (Germany), during October 2001 and 2002. A more detailed overview of the FEBUKO experimental design is given by Herrmann et al. (2005a), and the meteorological characterisation during the campaigns by Tilgner et al. (2005a) and Heinold et al. (2005). Hence, only a short description of the specific experimental set-up for particle and trace gases characterisation is given here.

Different collectors were applied to obtain samples for the chemical characterisation of particles. For the size-resolved particle sampling, BERNER impactors (BI, cut-offs: stage 1: 0.05–0.14, stage 2: 0.14–0.42, stage 3: 0.42–1.2, stage 4: 1.2–3.5, stage 5: 3.5–10 µm, aerodynamical particle diameter) were used which were conditioned at 60% RH to minimise bounce-off effects. Humidity was controlled by a sensor placed directly in front of the sampling inlet of the impactors and automatically regulated by changing the temperature of the sampling inlet line for each impactor. Two impactors, one with tedlar foil for major ion analysis and the other with aluminium foil for carbon analysis

(OC: organic carbon, EC: elemental carbon, TC: total carbon), were operated in parallel (flow volume: $75 \, l \, min^{-1}$). Additionally, ANDERSEN (HVA) for PM_{10} and DIGITEL (DF) high-volume filter samplers for PM_1 and $PM_{2.5}$ equipped with quartz fibre filter (Munktell MK 360) were used for high-volume samples (940, 300 and $500 \, l \, min^{-1}$, respectively). The total mass on the filter was determined using a microbalance. The filter samples were equilibrated 24 h at about 50% RH and 20 °C prior to weighing (Plewka et al., 2004). Recent study (INTERCOMP2000) shows a good agreement between the measurements using Munktell quartz fibre and other filters (Hitzenberger et al., 2004). The quartz fibre filter samples were used to identify and quantify organic particle constituents (Müller et al., 2005), some of water-soluble metals (Fe, Cu, Mn, and Zn), and for the comparison of mass and ion analysis. Furthermore, particles for anionic analysis were collected by the Steamjet (StJ) technique with online analysis by IC (Dionex), cf. Acker et al. (2003). The number size distribution of particles was measured by a Tandem Differential Mobility Particle Sizer (T-DMPS) for the particle size range between 3 and 900 nm. In the T-DMPS, particles were dried and classified at relative humidity below 10% (Birmili et al., 1999).

Standard trace gases mixing ratios (NO, NO_2, O_3, SO_2, and CO) were recorded by ambient trace gas monitors (Herrmann et al., 2005a). The concentrations of the trace gases (HCl, HONO, and HNO_3) were measured online by a Wet Effluent Diffusion Denuder (WEDD) using IC (Dionex) (Acker et al., 2001) and H_2O_2 by means of a H_2O_2-Analyser Model UD8801. The measured trace gas mixing ratios/concentrations are given in Table I (Electronic supplemental material, ESM), as well as a brief discussion of the temporal evolution during the events.

The collected particles were chemically analysed by ion chromatography (Metrohm) and capillary electrophoresis (Spectrophoresis1000) for the main ionic components (Brüggemann and Rolle, 1998; Neusüß et al., 2000a). OCEC was determined by a two-step thermographic method (C-mat 5500, Ströhlein), see Plewka et al. (2004). The metals in the BI and HVA samples were analysed using atomic absorption spectrometry (Perkin Elmer) (Chemnitzer, 2002; Rüd, 2003). Table II (ESM) lists the measured size-segregated concentrations for particulate mass, Cl^-, NO_3^-, SO_4^{2-}, Na^+, NH_4^+, K^+, Mg^{2+}, Ca^{2+}, OC, EC, water-soluble Fe, Cu, Mn, and Zn (PM_{10}). In addition, the sum of all impactor stages (corresponding to PM_{10}), the HVA PM_{10} concentrations and the total (without cut-off) concentrations of Cl^-, NO_3^- and SO_4^{2-} by StJ are shown.

Quality control was achieved through successful participation in international ring analysis initiatives by WMO-EPA each year since 1991 (http://www.marble.asrc.cestm.albany.edu/qasac/) for ion analysis.

The OCEC method used in this study was involved in the International Round Robin Test Carbon Shoot out Stage I (Schmid et al., 2001) and Stage II (Puxbaum, TU Vienna, unpublished) and in the INTERCOMP2000 campaign (ten Brink et al., 2004).

3. Results and discussion

A set of total 14 events from campaign 2001 and 2002 was selected for detailed analysis. The best conditions (defined by a connected flow upwind-summit-downwind site) were fulfilled during three events. These are E I: 26/27-October 2001, E II: 06–08-October 2001, and E III: 16/17-October 2002 (Tilgner et al., 2005a; Heinold et al., 2005). These events were chosen for further discussion. The complex data set of the particle and gas phase concentrations from the upwind site is used for the initialisation of the complex multi-phase chemistry model SPACCIM (Wolke et al., 2005) and its application with CAPRAM3.0 (Herrmann et al., 2005b; Tilgner et al., 2005b).

3.1. Particle mass

The total mass concentration of particles on the impactor foils (PM$_{10}$: sum of the five BI stages) based on gravimetric measurements amounts to between 8 and 17 µg m^{-3}. This is comparable to other measurements at rural sites in Germany and middle Europe (Table 1) but is lower than near-city measruements. For example, the PM$_{10}$ mean value in Melpitz was about 33 µg m^{-3} in 1995 (Müller et al., 2005) and the range during an autumn campaign in 1997 was found to be 13–47 µg m^{-3} (Neusüß et al., 2002; Plewka et al., 2004). For Waasmunster (B—July 1994–November 1995), a mean

value of 38 and for Ispra (I—February 2000–December 2000) of 29 µg m^{-3} was determined (Putaud et al., 2004). At urban sites, the PM$_{10}$ mean values were 24, 38, and 47 µg m^{-3} in Zurich (CH—January 1998–March 1999), Gent (B—May 1993–July 1994) and Bologna (I—2002), respectively (Putaud et al., 2004).

For E I and E II, a distribution of particle mass in the five BI size ranges was found (Fig. 1) to be a typical aged central European aerosol (Neusüß et al., 2000a, b). E III shows more maritime-influenced aerosol recognisable by elevated sea salt fractions in the coarse mode on stages 4 and 5 (Fig. 3). Ninety six hour backward trajectories of the sampled air masses were produced with HYSPLIT from the NOAA ARL Website (http://www.arl.noaa.gov/ready/), see Tilgner et al. (2005a).

Table 1
Mean PM$_{10}$ concentration for rural sites

Site	Period	PM$_{10}$ (µg m^{-3})
Westerland (G)	2001	20[a]
Zingst (G)	2001	17[a]
Neuglobsow (G)	2001	16[a]
Waldhof (G)	2001	16[a]
Schmücke (G)	2001	10[a]
Deuselbach (G)	2001	15[a]
Brotjacklriegel	2001	10[a]
Schauinsland (G)	2001	10[a]
Chaumont (CH)	Jan98–Mar99	11[b]
Monagrega (CH)	Mar99–Jul00	18[b]
Illmitz (A)	Oct99–Oct00	24[b]
Schmücke (G)	Oct01, Oct02	8–17[c]

[a]Beilke et al., 2002.
[b]Putaud et al., 2004.
[c]This work.
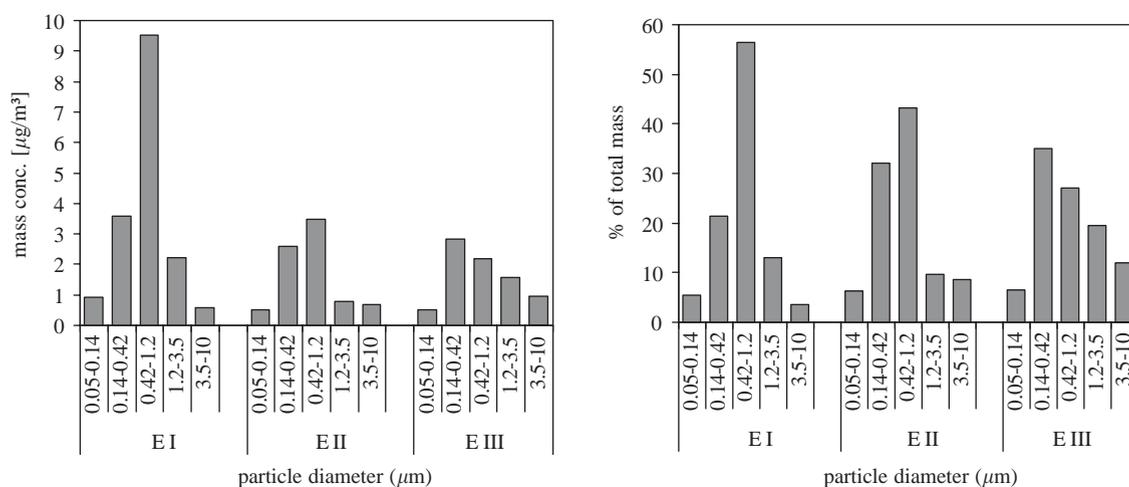
Fig. 1. Size-segregated mass concentration and percentage of stage mass to total mass concentration at upwind site.

Particle mass concentrations were measured also by DIGITEL (PM$_1$ in 2001/PM$_{2.5}$ in 2002) and a HVA filter sampler (PM$_{10}$). The comparison of all three samplers is presented in Fig. 2. BI (PM$_{1.2}$) vs. DF (PM$_1$) shows a reasonable agreement. A slight excess of the BI mass can be caused by the higher cut-off. The particle mass of BI (PM$_{3.5}$) vs. DF (PM$_{2.5}$) shows excess values of about 50% for the DF. Moreover, BI (PM$_{10}$) vs. HVA (PM$_{10}$) shows even an excess of $>100\%$ for the HVA. These differences could be attributed to positive and negative artefacts of the respective sampling techniques. Losses of volatile components by BI
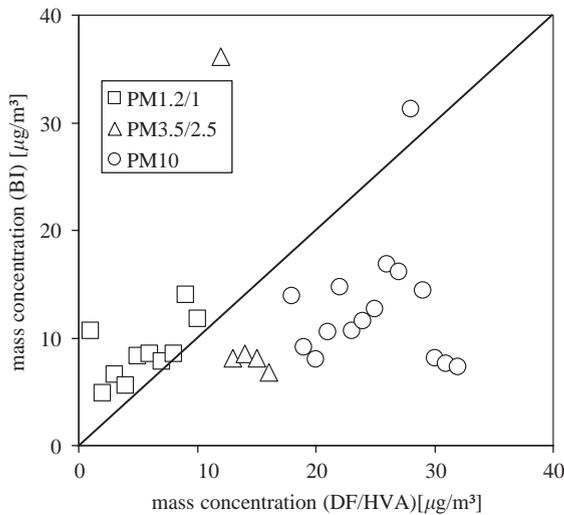
sampling cannot be fully excluded, especially for smaller particles, because of pressure drop (Neusüß et al., 2000a). Bounce-off effects in the upper stages of impactor might also contribute to mass losses (Wang and John, 1988; Hillamo and Kauppinen, 1991). Quartz fibre filters can adsorb gaseous components from the sample air stream forming excess mass (Cadle and Mulawa, 1990) and react with gaseous compounds (Zhang and McMurry, 1991). Additionally, high-volume filter samplers exhibit a much flatter curve of particle deposition efficiency (Schaap et al., 2004; Hitzenberger et al., 2004).

3.2. Ionic components

The total concentrations of major ionic components (summed up to PM$_{10}$) reach 6.55 (E I), 2.67 (E II) and 2.53 μg m^{-3} (E III). The total concentration of ion mass of E I is about twice higher than E II and E III. The contribution of ions to particle mass (PM$_{10}$) is about 40% (E I) and 30% (E II and E III). In Fig. 3, the concentrations of size-segregated main ionic components for the three events are presented. The major components are nitrate, sulphate, and ammonium (about 90% of the total ionic concentration).

For E I, the highest ionic concentration was found on stage 3 followed by stages 2, 4, 5 and 1. Nitrate has the highest concentration, followed by sulphate and ammonium with maximum on stage 3 (0.42–1.2 μm). The other components (Cl$^-$, Na$^+$, Mg^{2+}, Ca^{2+}) show the highest concentration (from sea salt and soil) on the stages 4 and 5 (1.2–10 μm) and stages 2 and 3 (0.14–1.2 μm) for K$^+$ (wood burning). In E II, the sulphate concentration was the highest on stages 3 followed by 2 and in E III on stages 2 followed by 3. The order of nitrate concentration was found to be stage $3>2>4$ for E I and II but it

Fig. 2. Comparison of mass concentration measured by BERNER impactor (BI—PM$_{1.2}$, PM$_{3.5}$, and PM$_{10}$), Digitel filter sampler (DF—PM$_1$ and PM$_{2.5}$), and High-Volume Andersen filter sampler (HVA—PM$_{10}$).
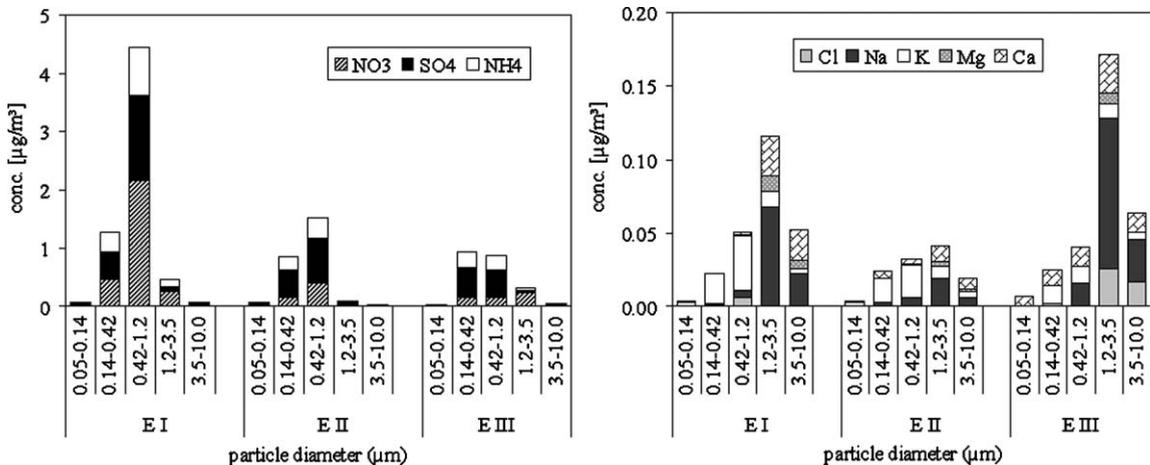
Fig. 3. Size-segregated particle concentration of main ion components for the three events at upwind site.
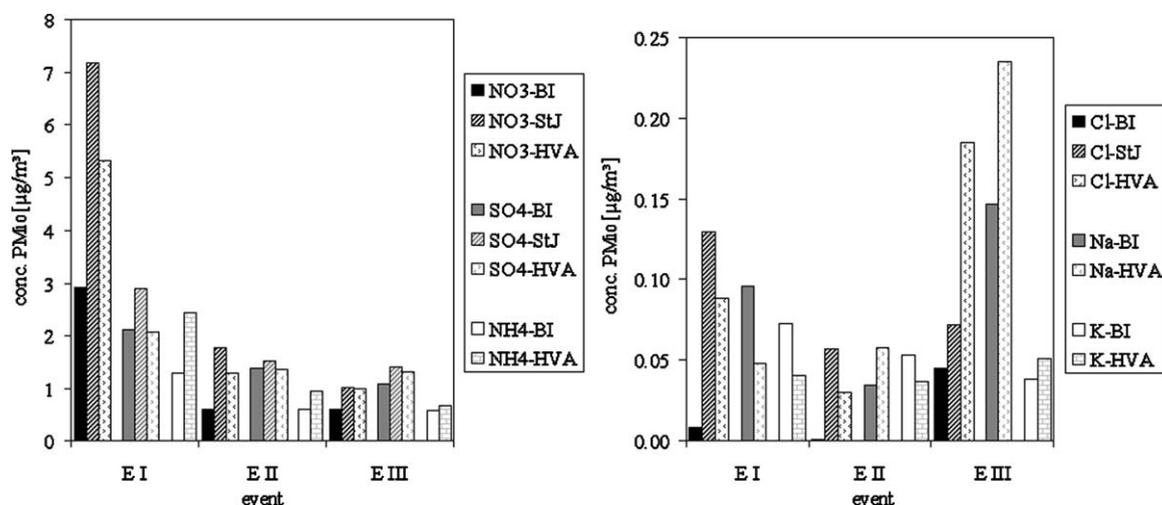
Fig. 4. Comparison of ion concentration (PM_{10}) measured by BERNER impactor (BI), Steamjet technique (StJ), and High-Volume Andersen sampler (HVA).

was in a reverse order for E III (stage $4 > 2 > 3$). Together with the very high concentrations of sea salts components (sodium, chloride, magnesium and calcium) on stage 4, it can be assumed that the aerosol for E III was of marine origin.

Fig. 4 shows the comparison for some ionic components measured by BI, HVA and StJ sampler (PM_{10}). It can be seen that there are some discrepancies between the samplers except for sulphate which is determined in relative good agreement for all three events. Differences can originate from different collection techniques, from contamination of the samples or inaccuracy in the chemical analysis. The analytical error for all components is on average below 10% but it can be as high as up to 50% near the detection limit.

The particulate concentration of chloride and nitrate was typically higher in the StJ than in BI samples. This is due to the sampling performance of StJ (denuded gases, particles are absorbed in water vapour without cut-off) excluding adverse effects as discussed for BI or HVA sampling. Based on StJ values, chloride found in BI samples was much lower and about 30% and 50% lower in HVA samples for E I and E II, respectively. In E III, the chloride loss for BI amounts to about 40% and for HVA an excess of 150% can be observed. The particulate chloride of the HVA samples minus the gaseous HCl concentration shows an excess of about 30%. This is an indication of a possible adsorption of gaseous HCl on the HVA filter sample (gaseous HCl concentration in E III is 4–8 fold higher than in E I and E II, see Table I—ESM). The discrepancies of nitrate concentration between the different samplers were about -60%, -70%, and -40% for BI and -25%, -25%, and 0% for HVA (all based on StJ) for E I, E II and E III, respectively. The measured particulate ammonium

concentrations from BI were about 50% (EI), 35% (EII), and 15% (EIII) lower than from HVA. However, it cannot be checked if there is a NH_4^+ loss for BI and/or an excess for HVA. Losses of ammonium nitrate during both filter and impactor sampling are discussed in Chang et al. (2000). The cations (Na^+, K^+, Mg^{2+}, and Ca^{2+}) cannot evaporate and do not have gaseous precursors in the atmosphere. The different concentration of these between BI and HVA samples in E III could be explained with the higher mass concentration sampled by HVA filter sampler, mainly in the larger particle size range (because of the flat collection efficiency curve), see Figs. 2 and 3. There is a possibility of contaminations from re-suspended soil materials (alkaline and alkaline-earth oxides and silicates).

In order to compensate the sampling errors the ionic concentrations of volatile components were adapted at the StJ values including the measured mass size distribution to initialise the model calculations, see Tilgner et al. (2005b) for further details.

3.3. OCEC

The carbonaceous particle fraction forms an important part of the aerosol mass. Considering PM_{10} (sum of all impactor stages), the fraction of TC in E I (12%) was lower than in E II (19%) and E III (18%). This was due to the smaller OC fraction during E I while the EC fractions were more or less constant during all three events between 5% and 6%.

Fig. 5 shows the measured OCEC concentration and the contribution to the mass on each impactor stage. The total OC concentration (PM_{10}) for all three events (E I, II and III) was about $1.0\,\mu g\,m^{-3}$. Total EC concentrations were 1.0, 0.45, and $0.40\,\mu g\,m^{-3}$ for EI, II
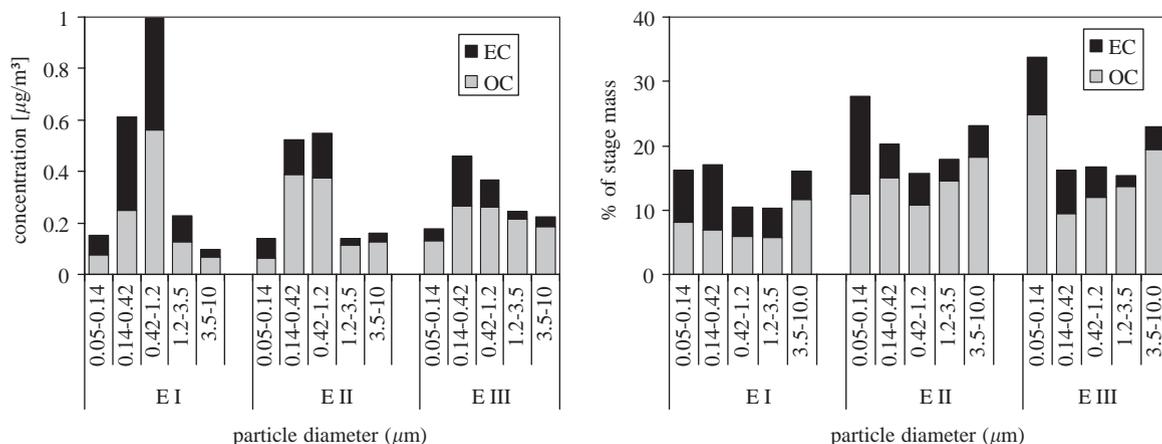
Fig. 5. Size-segregated OCEC concentration and the percentage of stage mass for the three events at upwind site.

and III, respectively. The total OC/EC ratios were 1.1 (E I), 2.4 (E II) and 2.6 (E III). Air masses of E II and E III showed similar OCEC values whereas E I showed smaller OC and lower EC/OC ratio than the other two events. The OC/EC ratio is an important parameter considering the activation of the particles as a CCN and cloud droplet formation (Mertes et al., 2005; Brügge-mann et al., 2005). OC influences particle growth or surface tension depending on its chemical composition. Therefore, the detailed analysis of OC fraction to determine most of organic single species is desirable (see Müller et al., 2005).

Size-segregated analysis for E I shows that a TC fraction accounts 16–17% on stages 1, 2 and 5 compared to only 10% on stages 3 and 4. E II and E III show their highest TC fraction on stage 1 with approximately 30% followed by stage 5 with 23%. TC fractions on stages 2 and 4 were in the range of 15–20%.

OC/EC ratios for E I were especially low in the range of 0.7–1.3 (except stage 5) as well as the stage 1 for E II. Low OC/EC ratios from small particles indicate fresh diesel vehicle emissions (Turpin and Huntzicker, 1995; Plewka et al., 2004) in the narrow valley of the upwind site possibly caused by lorries and cars of the inhabitants. One thing to note is that OC/EC ratios also may be influenced by different separation and analytical methods resulting in different OCEC fractions (Schmid et al., 2001; ten Brink et al., 2004). The fraction on stage 3 for E I indicates an aged air mass influenced by traffic and possibly industrial EC emissions. The E II air mass is more OC dominated (OC/EC = 2.8, 2.2, 4.4, 3.6; stages 2–5). The OC/EC ratio in E III rises up to 7.7 at stage 4 and 5.5 at stage 5. The OC/EC ratio generally increases during particle ageing. A part of aged organic materials is called secondary organic aerosol (SOA) formed by oxidised VOCs. Therefore, OC/EC ratios can be used to estimate SOA concentrations (e.g. Strader et al., 1999). Higher OC fractions in the coarse particle size

range ($PM_{1.2-10}$) can originate from biogenic (e.g. plant wax abrasion and pollen) or anthropogenic sources (tire abrasion and re-suspension). The differentiation can be performed using the Carbon Preference Index (CPI_{odd}), the ratio of odd and even alkanes (see Müller et al., 2005). In PM_{10} filter samples from E I and E II CPI_{odd} of about 0.9 were determined. This suggests anthropogenic sources (fuel alkanes) on the highest loaded stages but does not exclude fractions of biogenic alkanes on the coarse stages as found in other studies (Herrmann et al., 2005a, b).

3.4. Mass closure

Mass closure includes the comparison of the gravimetric mass determined by weighing the particle samples using a microbalance with the physically calculated mass or the chemically determined mass consisting of all components determined. Average particle number size distributions from events I, II, and III are discussed in detail and figures of volume and number size distributions are presented in Brüggemann et al. (2005) and Mertes et al. (2005).

3.4.1. Physical mass closure

The masses corresponding to each size range were calculated from the continuously measured dry particle size distributions by the procedure described in Neusüß et al. (2000b, 2002). The T-DMPS measured size distributions were averaged over the whole event time. Particle diameters at 60% RH are estimated from DMPS size distributions at 10% RH using growth factors (fg) derived from the simultaneously measured hygroscopic particle growth factor using a HTDMA (Hygroscopicity Tandem Differential Mobility Sizer) (Lehmann et al., 2005). From the mean dry particle number distributions the volume distributions were calculated using the wet diameters. The mass

distribution can be calculated from the volume distribution by means of the corresponding wet densities. For this purpose, wet densities were calculated from averaged dry densities (estimated from the compounds found by chemical analysis) using the growth factors: $\rho_{wet} = [(fg^3-1)/fg^3] \cdot \rho_{H_2O} + 1/fg^3 \cdot \rho_{dry}$. The used densities are: carbonaceous material (OM 1.65, EC 1.8), ions 1.7, unidentified fraction 2.2, and water $1.0\,g\,cm^{-3}$. The growth factors for 50, 150, and 250 nm particles, determined by a HTDMA, were found to be 1.08, 1.07, and 1.19 for E I; 1.07, 1.10, and 1.15 for E II, and 1.07, 1.08, and 1.11 for E III, respectively (Lehmann et al., 2005). The resulting mass distribution was integrated up to the corresponding impactor stage diameter. The wet size distribution corresponds roughly to the range up to 1 μm diameter, so the first three impactor stages can be compared.

Mass closure between BI and T-DMPS shows reasonable agreement (Fig. 6). The relative differences between calculated T-DMPS and BI mass concentrations are about −45%, 60%, and 50% for E I, −45%, 30%, and 50% for E II, and −60%, 10%, and 30% for E III on the size ranges of 0.05–0.14, 0.14–0.42, and 0.42–1.2 μm, respectively (positive bias means higher BI mass concentration). Neusüß et al. (2000b) found deviations of less than 10% to about 70% (often in the range of 30–40%) between gravimetric and number-derived mass concentrations due to measurement uncertainties.

3.4.2. Chemical mass closure

For the purpose of the chemical mass closure, the sum of OC has to be converted to organic mass (OM). OC to OM conversion factors between 1.2 and 2.6 were typically used, e.g. in Turpin et al. (2000). In this study, a conversion factor of 2.1 representing non-urban aerosol was applied (Turpin and Lim, 2001). A differentiation between the single size ranges (lower conversion factors for fresh fine particles and higher

Fig. 6. Mass closure between gravimetric determination and calculation of particle mass from the number size distribution.

factors for more coarse aged particles) was not considered because of insufficient knowledge of the chemical composition of OC fraction (about 15% are identified, see Müller et al., 2005).

The water content was estimated by the following approach (Neusüß et al., 2002): $m_{H_2O} = m_{dry}(((\rho_{wet}/\rho_{dry})f)-1)$ with m_{H_2O}—resulting water content, m_{dry}—chemical measured mass concentration, ρ_{wet}—density of wet particles, ρ_{dry}—density of dry particles, $f = (D_{wet}/D_{dry})^3$—volume growth factor (for spheric particles), $D_{wet,dry}$—diameter of wet or dry particles. As a first approximation, an average volume growth factor $(1.1)^3 = 1.33$ was used (Neusüß et al., 2000b). The density ratio ρ_{wet}/ρ_{dry} was estimated from the fractions of measured components. The value of ρ_{dry} was determined from fractions of compounds (NH_4NO_3 and $(NH_4)HSO_4$: $\rho_{dry} = 1.7\,g\,cm^{-3}$), OM (oxalate: $\rho_{dry} = 1.65\,g\,cm^{-3}$), EC (soot: $\rho_{dry} = 1.8\,g\,cm^{-3}$), and undetermined mass (SiO_2: $\rho_{dry} = 2.2\,g\,cm^{-3}$). The value of ρ_{wet} was calculated by the following approach: $\rho_{wet} = (1-(1/f))\ \rho_{H_2O} + (1/f)\rho_{dry}$. The water content was found to be in the range of about 16–18%. The mean hygroscopic growth factor derived from available measurements in the size range up to $D_p =$ 50, 150, and 250 nm was used also for more coarse particle fractions. Hysteresis effects could not be taken into account in this calculation. Therefore, results from this calculation are only approximate values. Nevertheless, this gives a rough idea on the water content of particle samples.

Size-segregated chemical mass closure for all events is shown in Fig. 7. The unidentified mass (UM) fraction from E I for all size ranges was higher than that of E II and E III. The percentage of UM for the three events was about 20% in average and as high as 50% for E I (stage 1). Such high fraction of UM, especially on the fine particle stages 1 and 2, was not observed from other measurement campaigns (e.g. Neusüß et al., 2002). In all events, stage 3 shows the lowest UM portion of about 10% which can be explained by crust material that was not analysed and possibly transported over long distances because of the long lifetime of such fraction. On stages 4 and 5, a higher portion of coarse particles (20–35%) produced by abrasion and re-suspension can contribute to the UM. Chemical analysis performed during the FEBUKO campaigns should be able to explain most of the mass fraction from fine particles (stage 1) as it is unlikely to contain crust materials such as silicates, silicon dioxide and metal oxides. However, higher UM portion (about 50%) from E I (stage 1) was observed and no explanation can be given at this moment. Investigations (joint project "Suspended dust" of IfT, Leipzig and Sächsisches Landesamt für Umwelt und Geologie, Dresden) from the size-segregated chemical composition of fine particles in Saxony including metal analysis by PIXE (Proton Induced X-ray Emission) show that these components amount only to a
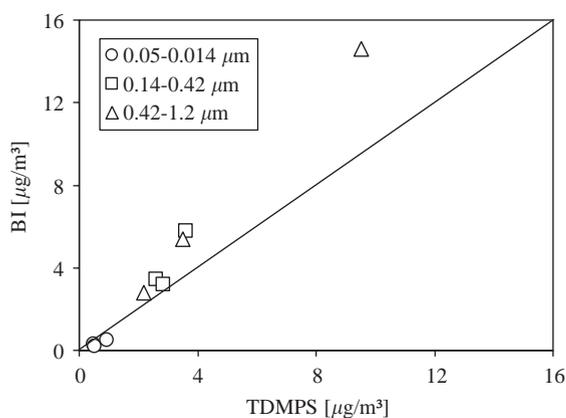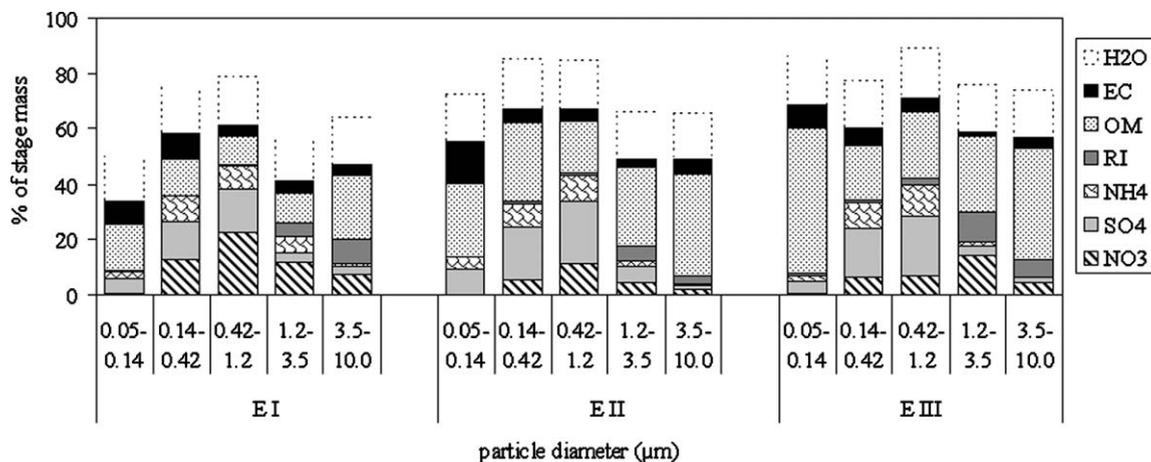
Fig. 7. Chemical mass closure (OM: organic material, RI: remaining ionic components).

minor portion on stage 1 and cannot be responsible for the large UM fraction. After all, the stage 1 mass of E I includes only 5% of the total sample mass and single components are only traces. Therefore, the 50% UM fraction amounts only to 3% of the total mass and does not contribute significantly to the total mass balance. Nevertheless, the chemical mass closure of particle components is quite well for the BI stages 2–5 (0.14–10 μm). The observed losses of volatile components (mainly nitrate) for BI measurements (Fig. 4, in comparison to StJ and HVA) lead to the conclusion that the part of UM fraction should be lower than that estimated by this method.

4. Summary

Detailed measurements of the gas and particle phase constituents allowed good chemical and physical characterisation of the air mass flow from the upwind site to the cloud-covered summit and to the downwind site.

The total mass concentration of particles (PM_{10}) measured by BERNER impactor was between 8 and 17 μg m^{-3} and is comparable to other measurements at rural sites. More than 80% of the PM_{10} mass consists of particles with a diameter below 1.2 μm. The comparison of mass concentration sampled by BERNER impactor (BI), high-volume DIGITEL (DF), and ANDERSEN (HVA) filter collectors shows a sufficient agreement with slight surplus of the BI (BI-$PM_{1.2}$/DF-PM_1) and excess values of about 50% for the DF (BI-$PM_{2.5}$/DF-$PM_{3.5}$) and >100% for the HVA (BI-PM_{10}/HVA-PM_{10}).

The total concentration of ionic mass of E I was about twice higher than from E II and E III. The major ionic components are nitrate, sulphate, and ammonium which amount to 90% of the total ionic concentration. In E I

nitrate had the highest concentration but in E II and E III sulphate was the dominant component. The comparison of particulate ionic concentrations measured by BI, HVA, and Steamjet technique shows great losses of volatile components (chloride, nitrate, and ammonium) from BI. The sulphate concentration was determined in relative good agreement by the different collectors.

The fraction of TC concentration in total mass concentration was lower for E I (12%) than for E II (19%) and E III (18%). The EC portion was about equal in all three events between 4% and 5%. The OC/ EC ratio was smallest for E I (1.1) but it was much higher for E II (2.4) and E III (2.6). In E II and E III, the air mass is more OC dominated indicating SOA formation at the small particles (0.05–0.14 μm).

The physical mass closures derived from T-DMPS results show sufficient agreement with gravimetrically determined mass concentrations from BI. The chemical mass closure of particle components is reasonably good for the size ranges 0.14/0.42/1.2/3.5/10 μm but in the fine particulate range (0.05–0.14 μm) the portion of unidentified material is very high, especially for EI and E II.

Based on the data presented here, a separate data set was provided for each chosen event to initialise the model calculations with all measured concentrations, see Tilgner et al. (2005b) for further details.

Appendix A. Electronic Supplemental Material

The online version of this article contains additional supplementary data. Please visit doi:10.1016/j.atmosenv. 2005.02.007.

References

Acker, K., Möller, D., Wieprecht, W., Auel, R., Kalaß, D., Tscherwenka, W., 2001. Nitrous and nitric acid measurements inside and outside of clouds at Mt. Brocken. Journal of Water, Air and Soil Pollution 130, 331–336.

Acker, K., Wieprecht, W., Möller, D., 2003. Distribution of reactive nitrogen compounds between atmospheric gas and aerosol phase. In: ten Brink, H., Baltensperger, U. (Eds.), Composition and Size Evolution of the Secondary Aerosol. EUROTRAC-2 Subproject AEROSOL Final Report, GSF Munich, pp. 197–203.

Bardouki, H., Liakakou, H., Economou, C., Sciare, J., Smolik, J., Ždimal, V., Elefteriadis, K., Lazaridis, M., Dye, C., Mihalopoulos, N., 2003. Chemical composition of size-resolved atmospheric aerosols in the eastern Mediterranean during summer and winter. Atmospheric Environment 37, 105–208.

Beilke, S., Berg, R., Bieber, E., Uhse, K., Wallasch, M., 2002. Jahresbericht 2001 aus dem Messnetz des UBA: Messungen von Feinstaub im Messnetz des Umweltbundesamtes. Texte 69/02, pp. 3–27 (ISSN 0722-186X).

Birmili, W., Stratmann, F., Wiedensohler, A., 1999. Design of a DMA-based size spectrometer for a large particle size range and stable operation. Journal of Aerosol Science 30, 549–553.

Brüggemann, E., Rolle, W., 1998. Changes of some components of precipitation in East Germany after the unification. Water, Air, and Soil Pollution 107, 1–23.

Brüggemann, E., Gnauk, T., Mertes, S., Acker, K., Auel, R., Wieprecht, W., Collett Jr., J.L., Chemnitzer, R., Rüd, C., Junek, R., Herrmann, H., 2005. Schmücke hill cap cloud and valley stations aerosol chemical composition during FEBUKO (I): Standard trace gases, main components and metals. Atmospheric Environment 123, 12 (this issue).

Cadle, S.H., Mulawa, P.A., 1990. Atmospheric carbonaceous species measurement methods comparison study: General motors results. Aerosol Science and Technology 12, 128–141.

Chang, M.C., Sioutas, C., Kim, S., Gong Jr., H., Linn, W.S., 2000. Reduction of nitrate losses from filter and impactor samplers by means of concentration enrichment. Atmospheric Environment 34, 85–98.

Chemnitzer, R., 2002. Bestimmung von Metallen in troposphärischen Partikeln und Wolkentröpfchen mittels Atom-Absorptionsspektrometrie. Diplomarbeit Technische Universität Bergakademie Freiberg.

Electronic supplemental material: (http://www.projects. tropos.de:8088/afo2000g3/FEBUKO_dateien/febuko.html/).

Hallberg, A., Noone, K.J., Ogren, J.A., Okada, K., Heintzenberg, J., Svenningsson, I.B., 1994. The influence of aerosol particle composition on cloud droplet formation. Journal of Atmospheric Chemistry 19, 153–171.

Hegg, D.A., Covert, D.S., Jonson, H., Khelif, D., Friehe, C.A., 2004. Observations of the impact of cloud processing on aerosol light scattering efficiency. Tellus 56B, 285–293.

Heinold, B., Tilgner, A., Jaeschke, W., Haunold, W., Knoth, O., Wolke, R., Herrmann, H., 2005. Meteorological characterisation of the FEBUKO hill cap cloud experiments, Part II: Tracer experiments and flow characterisation with nested non-hydrostatic atmospheric models. Atmospheric Environment (this issue).

Herrmann, H., Wolke, R., Müller, K., Brüggemann, E., Gnauk, T., Barzaghi, P., Mertes, S., Lehmann, K., Massling, A., Birmili, W.A., Wiedensohler, A., Wieprecht, W., Acker, K., Jaeschke, W., Kramberger, H., Svrcina, B., Bächmann, K., Collett Jr., J.L., Galgon, D., Schwirn, K., Nowak, A., vanPinxteren, A., Plewka, A., Chemnitzer, R., Rüd, C., Hofmann, D., Tilgner, A., Diehl, K., Heinold, B., Hinneburg, D., Knoth, O., Sehili, A.M., Simmel, M., Wurzler, S., Mauersberger, G., Majdik, Z., Müller, F., 2005a. FEBUKO and MODMEP: Field measurements and modelling of aerosol and cloud multiphase processes. Atmospheric Environment, this issue, doi:10.1016/j. atmosenv.2005.02.004.

Herrmann, H., Tigner, A., Barzaghi, P., Majdik, Z., Gligorovski, S., Poulain, L., Monod, A., 2005b. Towards a more detailed description of tropospheric aqueous phase organic chemistry: CAPRAM 3.0. Atmospheric Environment, this issue, doi:10.1016/j.atmosenv.2005.02.016.

Hillamo, R.E., Kauppinen, E.I., 1991. On the performance of the Berner low pressure impactor. Aerosol Science and Technology 14, 33–47.

Hitzenberger, R., Berner, A., Galambos, Z., Maenhaut, W., Cafmeyer, J., Schwarz, J., Mueller, K., Spindler, G., Wieprecht, W., Acker, K., Hillamo, R., Mäkelä, T., 2004. Intercomparison of methods to measure the mass concentration of the atmospheric aerosol during INTER-COMP2000—influence of instrumentation and size cuts. Atmospheric Environment 38, 6467–6476.

Kreidenweis, S.M., Walcek, C., Kim, C.H., Feingold, G., Gong, W., Jacobson, M.Z., Liu, X., Penner, J., Nenes, A., Seinfeld, J.H., 2003. Modification of aerosol mass and size distribution due to aqueous-phase SO_2 oxidation in clouds: comparisons of several models. Journal of Geophysical Research 108 (D7), 4213.

Lammel, G., Brüggemann, E., Gnauk, T., Müller, K., Neusüss, C., Röhrl, A., 2003. A new method to study aerosol source contributions along the tracks of air parcels and its application to the near-ground level aerosol chemical composition in central Europe. Journal of Aerosol Science 34, 1–25.

Lehmann, K., Massling, A., Tilgner, A., Mertes, S., Galgon, D., Wiedensohler, A., 2005. Size-resolved soluble volume fractions of submicrometer particles in air masses of different character. Atmospheric Environment, this issue, doi:10.1016/j.atmosenv.2005.02.011.

Maenhaut, W., Cafmeyer, J., Dubtsov, S., Chi, X., 2002. Detailed mass size distribution of elements and species, and aerosol chemical mass closure during fall 1999 at Gent, Belgium. Nuclear Instruments and Methods in Physics Research 189, 238–242.

Mertes, S., Galgon, D., Schwirn, K., Nowak, A., Lehmann, K., Massling, A., Wiedensohler, A., Wieprecht, W., 2005.

Evolution of particle concentration and size distribution observed upwind, inside and downwind hill cap clouds at connected flow conditions during FEBUKO. Atmospheric Environment, this issue, doi:10.1016/j.atmosenv.2005.02.009.

Mészáros, E., Barcza, A., Gelencsér, A., Hlavay, J., Kiss, G., Kriváscy, Z., Molnár, A., Polyák, K., 1997. Size distribution of inorganic and organic species in the atmospheric aerosol. Journal of Aerosol Science 28, 1163–1175.

Mészáros, E., Molnár, A., Ogren, J., 1998. Scattering and absorption coefficients vs. chemical composition of fine atmospheric aerosol particles under regional conditions in Hungary. Journal of Aerosol Science 29, 1171–1178.

Müller, K., van Pinxteren, D., Plewka, A., Svrcina, B., Kramberger, H., Hofmann, D., Bächmann, K., Herrmann, H., 2005. Aerosol characterisation at the FEBUKO upwind station Goldlauter (II): Detailed organic chemical characterisation. Atmospheric Environment (this issue).

Neusüß, C., Pelzing, M., Plewka, A., Herrmann, H., 2000a. A new analytical approach for size-resolved speciation of organic compounds in atmospheric aerosol particles: methods and first results. Journal of Geophysical Research 105 (D4), 4513–4527.

Neusüß, C., Weise, D., Birmili, W., Wex, H., Wiedensohler, A., Covert, D.S., 2000b. Size-segregated chemical, gravimetric, and number distribution-derived mass closure of the aerosol in Sagres, Portugal during ACE-2. Tellus 52B, 169–184.

Neusüß, C., Wex, H., Birmili, W., Wiedensohler, A., Koziar, C., Busch, B., Brüggemann, E., Gnauk, T., Ebert, M., Covert, D.S., 2002. Characterization and parameterization of atmospheric particle number-, mass-, and chemical-size distributions in central Europe during LACE 98 and MINT. Journal of Geophysical Research 107, 8127.

Nunes, T.V., Pio, C.A., 1993. Carbonaceous aerosols in industrial and coastal atmospheres. Atmospheric Environment 27, 1339–1346.

Pakkanen, T.A., Kerminen, V.M., Loukkola, K., Hillamo, R.E., Aarnio, P., Koskentalo, T., Maenhaut, W., 2003. Size distribution of mass and chemical components in street-level and rooftop PM$_1$ particles in Helsinki. Atmospheric Environment 37, 1673–1690.

Plewka, A., Gnauk, T., Brüggemann, E., Neusüß, C., Herrmann, H., 2004. Size-resolved aerosol characterisation for a polluted episode at the IfT research station Melpitz in Autumn 1997. Journal of Atmospheric Chemistry 48, 131–156.

Putaud, J.-P., Raes, F., van Dingenen, R., Baltensberger, U., Brüggemann, E., Facchini, M.-C., Decesari, St., Fuzzi, S., Gehrig, R., Hansson, H.-C., Hüglin, C., Laj, P., Lorbeer, G., Maenhaut, W., Mihalopoulos, N., Müller, K., Querol, X., Rodriguez, S., Schneider, J., Spindler, G., ten Brink, H., Törseth, K., Wiedensohler, A., 2004. A European aerosol phenomenology: 2. Chemical characteristics of particulate matter at kerbside, urban, rural, and background sites in Europe. Atmospheric Environment 38, 2579–2595.

Rüd, C., 2003. Bestimmung von Metallen in Aerosolpartikeln und Wolkenwasser mittels Atom-Absorptionsspektrometrie. Diplomarbeit Universität Leipzig.

Schaap, M., Spindler, G., Schulz, M., Acker, K., Maenhaut, W., Berner, A., Wieprecht, W., Streit, N., Müller, K., Brüggemann, E., Putaud, J.-P., Puxbaum, H., Baltensperger, U., ten Brink, H.M., 2004. Artefacts in the sampling of nitrate studied in the, INTERCOMP' campaign of EUROTRAC-AEROSOL. Atmospheric Environment 38, 6487–6496.

Schmid, H., Laskus, L., Abraham, H.J., Baltensperger, U., Lavanchy, V., Bizjak, M., Burba, P., Cachier, H., Crow, D., Chow, J., Gnauk, T., Even, A., ten Brink, H.M., Giesen, K.-P., Hitzenberger, R., Hueglin, C., Maenhaut, W., Pio, C., Carvalho, A., Putaud, J.-P., Toom-Sauntry, D., Puxbaum, H., 2001. Results of the "carbon conference" international aerosol carbon round robin test stage I. Atmospheric Environment 35, 2111–2121.

Strader, R., Lurmann, F., Pandis, S.N., 1999. Evaluation of secondary organic aerosol formation in winter. Atmospheric Environment 33, 4849–4863.

ten Brink, H., Maenhaut, W., Hitzenberger, R., Gnauk, Th., Spindler, G., Even, A., Chi, X., Bauer, H., Puxbaum, H., Putaud, J.-P., Tursic, J., Berner, A., 2004. INTERCOMP2000: the comparability of methods in use in Europe for measuring the carbon contnet of aerosol. Atmospheric Environment 38, 6507–6519.

Tilgner, A., Heinold, B., Nowak, A., Herrmann, H., 2005a. Meteorological characterisation of the FEBUKO hill cap cloud experiments, Part I: Synoptic characterisation of measurement periods. Atmospheric Environment (this issue).

Tilgner, A., Majdik, Z., Sehili, A.M., Simmel, M., Wolke, R., Herrmann, H., 2005b. SPACCIM: Simulations of multiphase chemistry occuring in the FEBUKO hill cap cloud experiments. Atmospheric Environment (this issue).

Turpin, B.J., Huntzicker, J.J., 1995. Identification of secondary organic aerosol episodes and quantitation of primary and secondary organic aerosol concentrations during SCAQS. Atmospheric Environment 23, 3527–3544.

Turpin, B.J., Lim, H.-J., 2001. Species contribution to PM2.5 mass concentrations: revisiting common assumptions for estimating organic mass. Aerosol Science and Technology 35, 602–610.

Turpin, B.J., Saxena, P., Andrews, E., 2000. Measuring and simulating particulate organics in the atmosphere: problems and prospects. Atmospheric Environment 34, 2983–3013.

van Pinxteren, D., Plewka, A., Hofmann, D., Müller, K., Kramberger, H., Svrcina, B., Bächmann, K., Jaeschke, W., Mertes, S., Collett Jr., J.L., Herrmann, H., 2005. Schücke hill cap cloud and valley stations aerosol chemical composition during FEBUKO (II): Organic compounds. Atmospheric Environment (this issue).

Wang, H.-C., John, W., 1988. Characteristics of the Berner impactor for sampling inorganic ions. Aerosol Science and Technology 8, 157–172.

Wolke, R., Sehili, A.M., Simmel, M., Knoth, O., Tilgner, A., Herrmann, H., 2005. SPACCIM: A parcel model with detailed microphysics and complex multiphase chemistry. Atmospheric Environment (this issue).

Zhang, X., McMurry, P.H., 1991. Theoretical analysis of evaporative losses of adsorbed or absorbed species during atmospheric aerosol sampling. Environmental Science and Technology 25, 456–459.